Characterization and Modeling of an RMS-DC Solid-State Thermal Converter

DV Nicolae
Department of Electrical and Electronic Engineering Technology, University of Johannesburg
Johannesburg, South Africa
dnicolae@uj.ac.za

E. Golovins
National Metrology Institute of South Africa
Pretoria, South Africa
egolovins@nmisa.org

Abstract— The Root Mean Square (rms) measurements of alternating signal of any waveform are frequently done by means of thermal transfer instruments. The principle of these thermal transfer instruments is to transfer the heating energy of resistive load to a temperature-sensing element. The DC output of the sensor reflects the amount of electrical power (ac or dc) applied to the input. The paper addresses the characterization and modelling of an RMS-DC thermal converter of a solid state technology type at various frequencies. The theoretical and simulation analysis is carried out to outline the factors influencing the transfer characteristics of the converter device in the dc and ac input regimes.

Keywords— Thermal converter, thermoelectric sensor, thermal transfer, solid state device

I. Introduction

The Root Mean Square value of an AC wave shape initially was known as "effective" value or "heating value"; in other words, AC RMS is the equivalent to the DC heating value of a particular waveform. Effective values measurements have been reported in early years [1], [2] based on electrodynamic instruments.

The principle of thermal transfer energy measurements based on thermocouple as a temperature sensor was reported in [3], [4]. Later-on, true rms converters have been introduced based on solid-state technology [5], [6], [9].

The transfer methods based on the use of thermal converters in the National Metrology Institutes (NMIs) were developed by Hermach [1], [8]. The classic thermal converter is made of a heater resistance and a thermo-sensor in thermal contact with the heater but isolated electrically and is commonly known as a single-junction thermal converter (SJTC) [2], [3], [8]. Recently, multi-junction thermal converters (MJTCs) [7], thin-film (planar) MJTCs and semiconductor (solid state) RMS sensors [9], [11], [13] have been developed and implemented as AC-DC transfer standards. In the MJTC design, modifications were made by adding more (up to several hundreds) thermal junctions (thermocouples connected in series, around a common heater) [17], [18]. The disadvantages of the MJTC originate from its fabrication complexity. Then these standards were further modified by laying the heater resistor and thermocouples metal on thin-film technology on the silicon wafer [11]. The evolution of thin-film planar MJTCs is in the process of active research [17], [18]. Most commercial solid-state thermal transfer standards have thermal converters based on transistor/diode sensors which are more robust to overloading and electrostatic discharge [11], [13] [18].

II. Principle of Thermal Conversion

The RMS of an AC signal and the equivalent dc signal applied to the input should generate the same output in a perfect device. The RMS value assigned to an AC signal is the amount of the DC signal required to produce equivalent amount of heat on the same load. In accordance to the RMS definition, the AC signal is compared with the DC signal by alternately applying them to the same heater and measuring the temperature rise. Mathematically, it involves squaring the signal, taking the average and obtaining the square root. For any form of voltage signal $v(t)$, the basic definition of the true RMS conversion is [4], [6]:

$$V_{RMS} = \sqrt{\frac{1}{T}\int_0^T v^2(t)dt} \tag{1}$$

Based on this definition a few solutions exist at present:

- Rectification and scaling that is mostly applied for periodic sinusoidal signals.
- Analog integrator circuit where the integration depend on an additional capacitor. Hence it has problems for low frequencies as well as for high frequencies.
- Thermal AC-DC converter – as studied in this paper.

Fig. 1 shows the basic principle of a thermal converter. The method compares the heating response of an unknown AC signal to the heating response of a known DC reference, which is calibrated in the laboratory to an SI-traceable standard.
In steady state, the active power (P_1) dissipated by Heater 1 (R_1) is radiated ($\hbar\upsilon$) to temperature sensor 1 (S_1).

$$\begin{aligned} p(t) &= R_1^{-1}v^2(t) = \left(2V_{rms}^2 / R_1\right)\sin^2(\omega t) \\ P_1 &= \frac{1}{T}\int_0^T p(t)dt = V_{rms}^2 / R_1 \end{aligned} \tag{2}$$

The power dissipated on Heater 2 is:

$$P_2 = V_{DC}^2 / R_2 \tag{3}$$

The signal/temperature generated by S_1 is then compared and adjusted to null with that coming from Heater 2/Sensor 2. When the elements heater/sensor 1 are identical with heater/sensor 2, then in steady state the output DC voltage is equal to the input rms voltage:

$$V_{DC} = V_{rms} \tag{4}$$

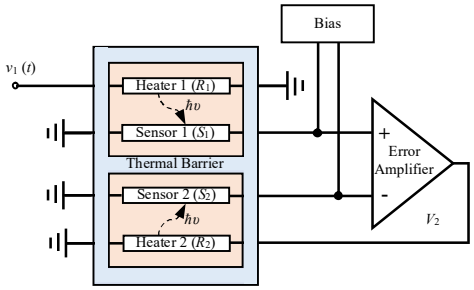

Fig. 1. Thermal RMS conversion – basic principle

A. Errors affecting thermal converter

There are many causes for AC-DC transfer difference:

- The main source of errors is mismatching of parameters of the two sections of the device.
- One other source of errors could be the thermal coupling between the sections. The entire derivation is based on presumption of the two sections being two adiabatic systems meaning no heat exchange between them.
- Thermoelectric effect (DC offset): passing of the DC signal through the heater of an RMS-DC thermal converter results in non-joule heating/cooling due to Thomson and Peltier effects. This produces a frequency-independent offset in the AC-DC difference [7], [15].
- High-frequency characteristic: The significance of the skin and proximity effects is observed at high frequencies, the alternating signal is confined to surface regions of the heater and not distributed uniformly across it. Therefore, the reactive components of the heater influence power dissipation within it when it is carrying a high-frequency alternating signal [7], [15].
- Low-frequency characteristic: double-frequency thermal ripple is expected at the output of the RMS-DC thermal converter [7], [15].

B. Heaters characterisation

In early years [1], [2], [3], when the measurements were of interest up to 20 kHz, the heater was in a form of resistive wire with relatively low inductive component. The moment higher frequencies came under scrutiny, the inductive part of the heater increased as well as skin effect; the heater became an impedance depending on input frequency signal.

The solution was building the heater within thin film technology and U geometry to reduce inductivity [17], [18] and using resistive materials with low temperature coefficient such alloys base of Cu & Ni.

C. Temperature sensor characterisation

Thermocouple was first temperature sensor used. It has good linearity and sensitivity of up to 68 μV/°C with relative low stability in time. Thermocouple provides a direct conversion between temperature and voltage.

The advent of thin-film technology did see introduction of "multi-junction" [9], [11], [13] meaning a large number of thermocouple have been connected in series increasing the sensitivity. Further research presented in [17], [18] shows introduction of 64 Si-Bi micro-thermocouples deposited on a polyimide film in conjunction with a NiCr heater sputtered on a 2 × 8-mm AlN chip.

Diode Semiconductor technology (Fig. 2) have been used due to temperature dependency of the voltage (V_D) upon ***p-n*** junction:

$$V_D = n\frac{k\theta}{q}\ln\left(1+\frac{I}{I_s}\right) \tag{5}$$

where n is "diode ideality factor", θ-the absolute temperature (°K), k-Boltzmann's constant, q-electron charge, I- biasing current (kept constant) and I_s-saturation current [19]:

$$I_s = qA\left(\frac{n_i^2}{N_D}\sqrt{\frac{D_p}{\tau_p}}+\frac{n_i^2}{N_A}\sqrt{\frac{D_n}{\tau_n}}\right) \tag{6}$$

where: q is electron charge; A-cross section area; $D_{p,n}$-diffusion coefficient at n side and p side respectively; $N_{D,A}$-are the donor/acceptor concentrations at n side and p side respectively; n_i-intrinsic carrier concentration in semiconductor material; $\tau_{p,n}$-are the carrier life times of holes and electrons respectively.

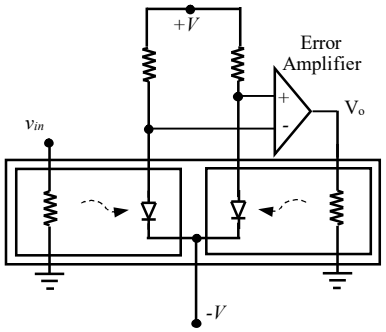

Fig. 2. Diodes-based Thermal RMS conversion

Saturation current increases much faster with temperature creating a negative temperature coefficient for diode forward voltage. The temperature coefficient for Si diode forward voltage is -2.5 mV/°C which few orders of magnitude higher than thermocouple.

Transistor is another solution to be used for temperature sensor (Fig. 3). The base current has a similar temperature dependency like diode, but due to current gain the sensitivity is higher than diode.

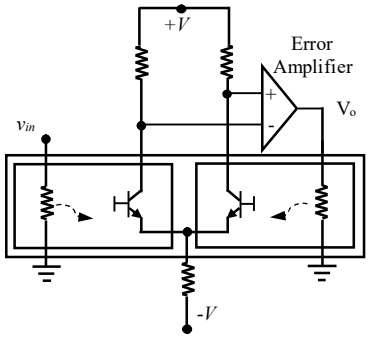

Fig. 3. Diodes-based Thermal RMS conversion

The main drawback of using diodes and/or transistors consist in high non-linearity temperature dependency. This drawback was solved by using two pairs heater/semiconductor sensor in a closed feedback loop [11], [12]. The good performances reported special in [13] were achieved by close matching transistors and resistance of heaters.

D. Thermal barrier

The low-temperature co-fired ceramics or glass-ceramics are used to package the two heater-sensor of the model - to prevent thermal cross-coupling between the sensor dies and minimize thermal exchange with the ambient [11].The die is isolated by vacuum or air from the package walls to provide the best thermal resistance and thus prevent heat flux losses [15].

III. MODELLING OF THERMAL CONVERTER

Considering all the above, in this study a dual heater/sensor topology in a closed loop was used.

A. Thermal modelling

Fig. 4 shows the simplified thermal equivalent diagram of one pair heater/die of temperature sensor. Parameter P_{in} is the thermal power generated by the electrical signal applied to the heater (v^2/R_H); $R_{th\text{-}heater}$ is thermal resistance of the heater; $C_{th\text{-}heater}$ is thermal capacitance of the heater; θ_{heater}-temperature of the heater; $R_{th\text{-}die}$- thermal resistance of the die; θ_{die}-sensor temperature; $C_{th\text{-}die}$ - thermal capacitance of the sensor; $R_{th\text{-}barrier}$ –thermal resistance of the barrier; $\theta_{ambiant}$ – ambient temperature.

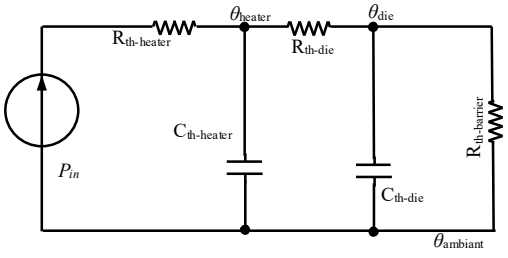

Fig. 4 Simplified thermal model

For dynamic analysis, the model was further simplified neglecting thermal barrier resistance (taken infinite) and the process can be described by a differential equation [14]:

$$mc\dot{\theta} + a\theta(t) = a\theta_{amb} \cdot u(t) + P_{in} \cdot u(t) \tag{7}$$

where mc is the caloric capacitance (C_{th}), a is the invers of thermal constant (τ_{th}), P_{in} –input power, θ_{amb} – ambient temperature and $u(t)$ is the "step" function.

$$a = \frac{hA}{mc} \tag{8}$$

where h is heat transfer coefficient through A area to the heated mass.

Calculating Laplace transform for (7) we get the temperature in Laplace domain:

$$\theta(s) = \frac{P_{in}}{mc} \cdot \frac{1}{s(s+a)} + \theta_{amb} \frac{1}{s} \tag{9}$$

Which in time domain becomes:

$$\theta(t) = \frac{P_{in}}{hA} \cdot \left(1 - e^{-at}\right) + \theta_{amb} \tag{10}$$

B. Matlab modelling

Based on thermal analysis and applying data for "diode" thermal converter [11], a Matlab/Simscape model was built. Fig. 5 and 6 show the simulation model of the RMS-DC solid state thermal converter. The model design assumes that the electrical input-output leakage (i.e. common mode noise) is absent. Since the technology of the matched pair of the thermo-resistive sensing elements is implemented inside the standard integrated circuit package, the state-of-the-art principles of the thermal effect modelling are applied to describe the heat transfer between the heater metal and semiconductor diode

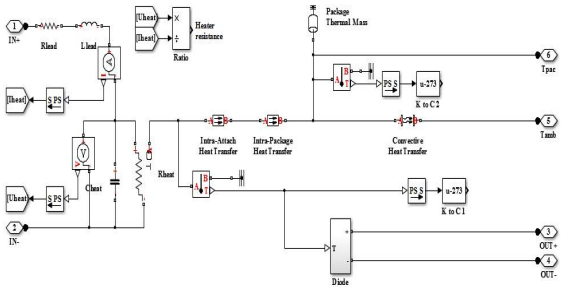

Fig. 5. Heater-sensor network diagram

The realised model capitalises on the electrical and thermal parameters extracted from [11]. The heater is a 50 Ω resistor with the known temperature coefficient (α = 0.002 1/K that identifies heater metal as brass having thermal conductivity 109 W/(m·K), specific heat capacity 380 J/(kg·K) and density 8500 kg/m3) that shares the die hosting the sensing diode(s) [11]. The thermal resistor parameters are determined using the

thermal equilibrium (steady state) equality under the maximum input power [14].

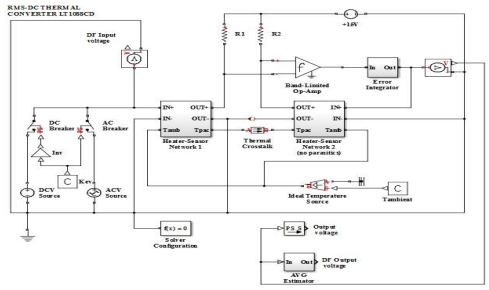

Fig. 6: Simscape simulation model of RMS-DC solid state thermal converter

The thermal sensor die is modeled as silicon due to both higher thermal conductivity (130 W/(m·K)) and higher specific heat capacity of 700 J/(kg·K) that yields larger thermal time constant. The diode junction is microscopic and has no thermal mass; thus the assumption holds that it gets heated immediately when the heat flux reaches it. The diode is a non-linear thermo-resistive element, and resistances of the metal lead tracks, which terminate at the diode pads and carry direct current, do not depend on the die temperature fluctuations, i.e. they can be excluded from the thermal network model. The low-temperature co-fired ceramics or glass-ceramics are used to package the two heater-sensor of the model - to prevent thermal cross-coupling between the sensor dies and minimise thermal exchange with the ambient [16]. The die is isolated by vacuum or air from the package walls to provide the best thermal resistance and thus prevent heat flux losses [13]. The air impregnated polymer layer is used to attach the die to the cavity bottom. This layer has a relatively high thermal resistance [11], [16].

IV. Simulation Results

The first set of simulation was to validate the frequency response and the heater-sensor temperature. Figure 7 shows the behaviour of the RMS-DC solid state thermal converter at the DC mode.

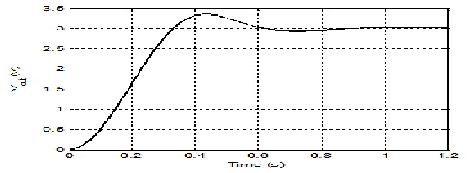

(a)

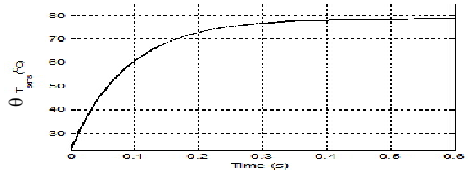

(b)

Fig. 7: DC response of the RMS-DC solid state thermal converter, (a) Output voltage, (b) Heater temperature

Figures 8, 9 and 10 show the response for a sinusoidal 3 $V_{RMS\text{-}in}$ at 10 Hz, 50 Hz and 100 Hz respectively.

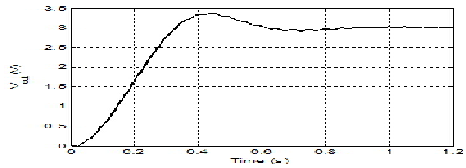

(a)

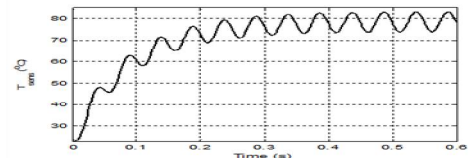

(b)

Fig. 8: 10 Hz response of the RMS-DC solid state thermal converter, (a) Output voltage, (b) Heater temperature

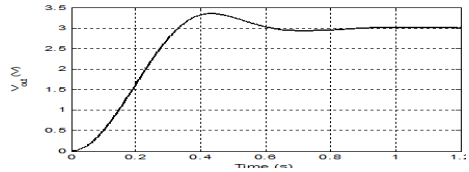

(a)

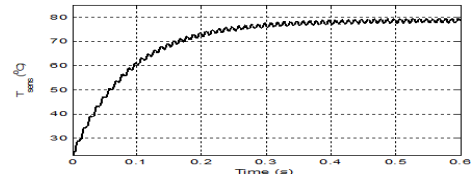

(b)

Fig. 9: 50 Hz response of the RMS-DC solid state thermal converter, (a) Output voltage, (b) Heater temperature

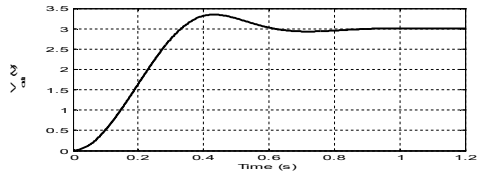

(a)

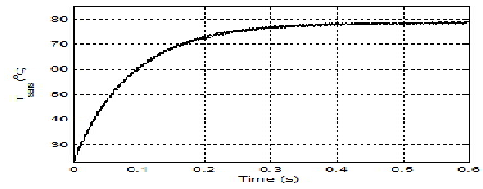

(b)

Fig. 10: 100 Hz response of the RMS-DC solid state thermal converter (a) Output voltage, (b) Heater temperature

The simulation results analyse the frequency response and heater temperature of the RMS-DC solid state thermal converter. The converter under study settles to a valid voltage output very quickly with negligible drift when compared to a thermocouple-based converter. The transient thermoelectric effects are observed by the ripple of the output voltage before settling to a constant value. The fast settling output voltage is produced by the small physical size of the RMS sensor, and the close matching of the two sections of the chip and the error integrator at the output of the thermal converter.

When a direct signal is applied to the input of the heater, the heater of the RMS-DC solid state thermal converter reaches a constant temperature. When an alternating signal (sinusoidal voltage) of frequency f is applied to the RMS-DC solid state thermal converter, joule heating in the thermal network varies with a double frequency, $2f$ [6], [14]. The temperature of the heater varies cyclically around the mean value, with amplitude which decreases with an increasing input frequency.

Provided that the input signal and the thermal network output are directly proportional to each other, the true RMS value of the AC signal can be determined by equating the mean of the varying heater temperature to the constant voltage of the DC reference. Nonlinearities in the direct proportional relationship will result in errors in the RMS value, i.e. the greater the nonlinearities the larger the errors. Any slight departure from the direct relationship of the input signal and output signal will have a slight effect on the AC-DC transfer difference when the double frequency thermal ripple is small. The reactive components of the heater influence how the signal is dissipated within it when it is carrying a high- frequency AC signal. The described responses depend on conditions that must be realized while the RMS-DC converter is designed.

The second set of simulation was to validate the true rms-dc conversion of the thermal converter. Figures 11 and 12 show the response of the 3 $V_{RMS\text{-}in}$ square wave and the sinusoidal signals at 10 Hz and 50 Hz respectively. It is observed that the RMS-DC solid state thermal converter maintains the same response for both the sinusoidal and square waveform input. Thus, the RMS-DC solid state thermal converter provides true RMS-DC conversion regardless of the input waveform.

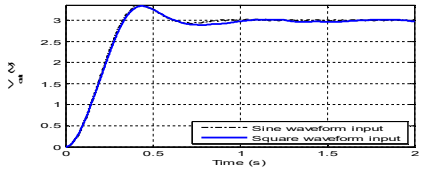

Fig. 11 Thermal converter response for 10 Hz sinusoidal and square wave

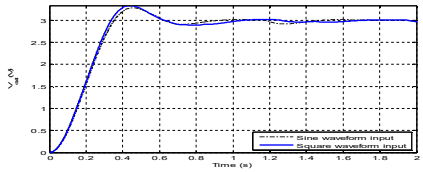

Fig. 12 Thermal converter response for 50 Hz sinusoidal and square wave

Figure 13 shows the plot of the linearity error of the RMS-DC solid state thermal converter, where:

$$\text{Linearity error} = \left| \frac{V_{in} - V_{out}}{(V_{in})_{max}} \right| \times 100\% \qquad (7)$$

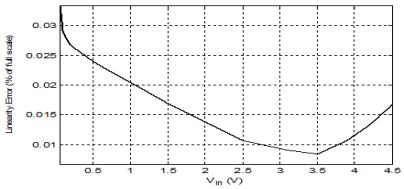

Figure 13: Linearity error of the RMS - DC Solid-state thermal converter: 0 V- 4.5 V

It is observed that the error due to nonlinearities in the RMS-DC solid state thermal converter is very small. Thus, the temperature rise of the heater can be used to accurately measure the RMS alternating signal.

In the determinations of the AC-DC transfer difference of the RMS-DC solid state thermal converter at higher frequencies, the skin effect of the heater, the stray inductance and capacitance at the device input are significant. Based on the definition of the AC-DC transfer difference, the AC and DC voltage are compared by the thermal method. Figure 12 shows the input and output AC-DC difference of the RMS-DC solid state thermal converter at higher frequencies.

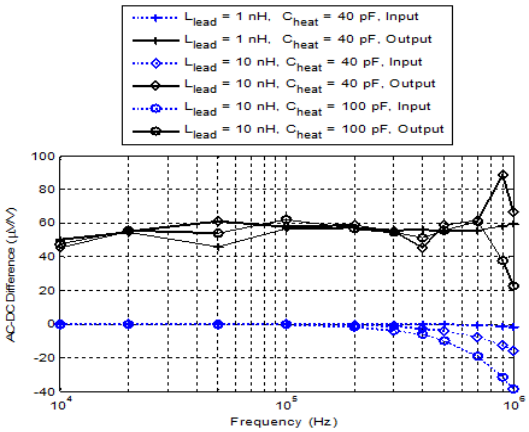

Figure 14: The input and output AC-DC transfer difference of the RMS-DC solid state thermal converter

When equal amount of AC and DC voltage is applied to the input heater of the thermal converter, the output response is expected to be equal for both inputs. However, due to the effect of non-joule heating and frequency characteristics of the heater of the thermal converter, the difference is observed between the output responses. The AC or DC signal can be adjusted in order to obtain the equal output response for both signals. The RMS-DC solid state thermal converter has negative AC-DC transfer difference at the input, which signifies that a larger amount of DC than AC is required by the RMS-DC solid state

thermal converter to operate at the same output level for both AC and DC signals.

V. Conclusions

In this paper an RMS-DC solid state thermal converter has been characterised, analysed and thermal & mathematically modelled. It was simulated at various frequencies and the results were presented and discussed. The analysis carried out in the paper outlines different factors which the errors affecting a thermal converter under calibration depend on.

Mathematic modelling was developed for better description of the thermal RMS converter operation and performances. The solid-state thermal converter offers many advantages such as short time constant and better frequency response compared to thermocouple-based thermal converters, Furthermore the solid-state thermal converter possesses linear input-output response, hence, the solid-state thermal RMS sensor is a practical alternative to single and multi-junction Thermal Voltage Conversions in all AC-DC difference applications.

References

[1] JH Park and AB Lewis, "Standard electrodynamic wattmeter and ac-dc transfer instrument", *Journal of Research of the National Bureau of Standards* 25, 545 (1940) RP 1344

[2] FL Hermach, "A precision electrotermic voltmeter for measurements between 20 and 20000 cycles", *Trans. Am. Inst. Elec. Engrs*. 67, 1224 (1948)

[3] WN Goodwin Jr., "The compensated thermocouple ammeter", *Trans. Am. Inst. Elec. Engrs*. 55, 23-33 (1936)

[4] F.L. Hermach, "Thermal converters as AC-DC transfer standards for current and voltage measurements at audio frequencies", *Journal of Research of the National Bureau of Standards*, Research Paper, Vol.48, 2296, No.2, February 1952

[5] L Marzeta, "Design Features of Precision ac-dc Converter", *Journal of Research of the National Bureau of Standards*, 73C-3, 4, 1969

[6] H Handler, "A Hybrid-Circuit RMS Converter", *Proceedings of the IEEE Solid-State Circuits Conference*, pp. 190-191, Feb. 1971

[7] FJ Wilkins, "Theoretical analysis of the AC-DC transfer difference of NPL multi-junction thermal converter over frequency range DC to 100 kHz", *IEEE Trans. on Instrumentation and Measurements*, vol. IM-21, pp. 334-340, Nov. 1972

[8] LF Hermach, "AC-DC comparators for audio-frequency current and volatge measurements of high accuracy, A survey of AC-DC Transfer Instruments and Basic Standards", *IEEE Trans. on Instrumentation and Measurements*, vol. IM-25, pp.489-496, Dec 1976

[9] LL Szepesi, "Recent developments on solid-state thermal converters", *Proc. Measurements Science Conference*, Irvine CA, pp. 9-13, January 1986

[10] C Kitchin and L Counts, "RMS-DC conversion", (Application guide), 2nd Edition, Section 1, pp. 2-3, 1986

[11] J. Williams, "A monolithic IC for 100 MHz RMS-DC conversion", (Application Note 22. AN22-4), September 1987

[12] Fluke 792A, "AC/DC transfer standard", Instruction Manual, 1990

[13] M. Klonz, "Current developments in accurate AC-DC transfer measurements", *IEEE Transactions on Instrumentation and Measurement*, Vol.44, No.2, April 1995

[14] MA Davies and TL Schmitz, *System Dynamics for Mechanical Engineers* (Chapter 9: Thermal Systems, pp 289-312), 2005

[15] Nano-Electronics Research Institute/AIST, Japan, A guide for establishing primary AC-DC transfer, *Tentative Version 2.01*, pp. 10-20, 12/April/2007

[16] Prof. Dr.-Ing. Jurgen Wilde, *Lecture Notes for assembly and packaging technology*, Laboratory for assembly and packaging technology, 2012

[17] T Lipe, "50-Ω Multijunction Thermal Converters on Fused Silica Substartes", *Conference on Precision Electromagetic Measurements*, pp. 44-45, 2014

[18] H Fujiki, Y Amagai, K Shimizume, K Kishino, and S Hidaka, "Fabrication of Thin Film Multijunction Thermal Converters With Improved Long-Term Stability", *IEEE Transactions on Instrumentation and Measurement*, Vol. 64, No. 6, June 2015

[19] TF Bogard, *Electronic Devices and Circuits*, Merill Publishing Company, 1986.